3160 J. Phys. Chem. 1993, 97, 3160–3165

Effect of Protonation on the Molecular Structure and Reactivity of a Typical Merocyanine Dye: Experimental and Theoretical Investigation

Shakir T. Abdel-Halim* and Mohamed K. Awad

Department of Chemistry, Faculty of Science, Tanta University, Tanta, Egypt

Received: April 27, 1992

The molecular reactivity of 1-methyl-2-(4-hydroxystyryl)pyridiniumbetaine (M) is affected upon protonation in both ground and excited states. In aqueous solution, the protonated trans form is photochemically active and isomerizes to give the cis form. The quantum yields ϕ_{tc} and ϕ_{ct} are determined. The rate constant and the thermodynamic parameters of the reverse cis → trans thermal reaction, from the unprotonated cis form, are also calculated. Due to the irreversibility of the thermal reaction, a complete molecular reaction cycle is performed in one direction. The excited molecule exhibits more acidic character than in the ground state. To correlate with the experimental work, ASED-MO calculations are applied for both unprotonated and protonated forms. The photochemical isomerization and the thermal reactions are discussed in terms of changes of the geometrical structure from the quinonoid to the benzenoid form upon protonation in both ground and excited states. Upon excitation, it seems that the molecular polarity character decreases in the case of M but increases for MH^+. Protonation is found as an exothermic, downhill reaction in the ground state and as an endothermic, uphill reaction in the excited state. It is shown that the lowest electronic transition is $\pi \rightarrow \pi^*$ which is higher for MH^+ than for M.

Introduction

Merocyanine dyes are heterocyclic compounds that have been extensively studied with interest due to their applications in a number of areas. They are used as electrochromic compounds for membrane potentials and high-voltage sensitivity.[1,2] Due to their charge asymmetry and molecular hyperpolarizability in nonlinear optics, they are exploited for laser doublers and liquid crystals.[3] The reactivity of photoisomerization of some merocyanine compounds is used for its potential applicability in generating erasable photomemory systems.[4] Other merocyanines have been reported as photoelectrochemical compounds[5] and photosensitizers.[6] Sieber et al.[7] recently reported that merocyanine 540 has been investigated to develop the phototherapy of leukemia through the leukemic cells. Other studies are devoted to use merocyanines for solar energy conversion as thin films or monolayers on glass substrates.[8,9]

Merocyanine of stilbazolium betaines have been found to be of more interest among the other merocyanine dyes because of their extreme solvatochromic properties.[10,11] Merocyanine dye M was synthesized and its solvatochromism was studied by us.[12] The long wavelength absorption and fluorescence band maxima exhibit strong negative solvatochromism. The variations of the solvatochromic absorption and fluorescence energies shift with solvent polarity in ten different polar solvents are 15 and 6 kcal/mol, respectively. Two linear correlations were found for the absorption and fluorescence energies with Dimroth–Reichardt,[13] ET(30). Also, the strong change of absorption and fluorescence energies of M are explained to be linearly multiple-parameters correlated with Taft's π^*[14-16] (nonspecific solvent polarity) and α[15] (hydrogen bond donor ability).[12] Increase of the negative solvatochromism of M is suggested as a result of decrease of its dipole moment upon excitation and increase of its ground-state dipole moment as a result of solvent polarization.[17a,b]

Change of molecular charge distribution of merocyanines upon solvation could be invoked to suggest that the increase of solvent polarity should alter the intercharge distribution of M from a quinonoid structure M_q (Scheme I), which exists more in nonpolar solvents, to a highly polar benzenoid structure M_b, which exists more in polar solvents.[18-21]

Several literature studies have shown that the valence structure of a conjugated π-electron system should be altered by protonation.[19,22-26] Consequently, protonation of the oxygen atom of M alters the quinonoid structure to the benzenoid structure. This is concomitant with a change in its protolytic and spectroscopic properties. The previous study concluded that the interaction of protic polar solvents with the oxygen atom of M, forming a H-bond, as well as its dielectric polarization cause the strongest absorption and fluorescence blue shifts.[12] The protonated benzenoid structure of M, the stilbene-like structure MH_b^+ (see Scheme I), leads to the possibility of proceeding the photochemical trans → cis isomerization. Other merocyanines have been investigated showing that the protonated structure is photoisomerically active in polar solvents.[27-29]

SCHEME I

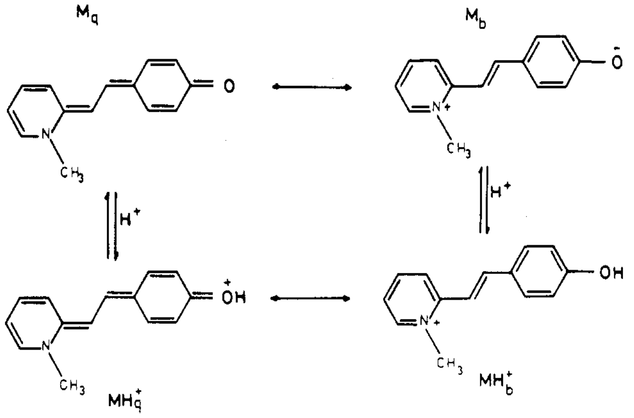

We report in this paper the role of protonation on the protolytic behavior of M in aqueous solution. The evidence to prove the effect of protonation on the electronic charge distribution and the molecular geometry was provided by studying the change of its absorption and fluorescence spectra, the possibility of photochemical trans → cis isomerization around the C═C bond, and the reverse thermal reaction. A theoretical study was also applied using ASED-MO calculations to correlate with the experimental results and to provide evidence for the effect of protonation of M on the molecular charge distribution and the equilibrium geometry, especially the stability of the olefinic bond in both ground and excited states. The nature of the different

0022-3654/93/2097-3160$04.00/0

electronic absorption transitions was also theoretically studied for M and MH$^+$ forms.

Experimental Section

(a) Materials and Instrumentation. The merocyanine dye M was synthesized according to procedures described in the literature.[30] It was recrystallized several times from water containing traces of KOH. Its purity was checked by thin-layer chromatography on aluminum oxide (neutral) and silica gel 60 F_{254} (Merck) and by elemental analysis. Organic solvents (Merck) were of reagent grade and used without further purification. For p*K* determination, buffer KH_2PO_4 (Merck) and NaOH (1 N titrisol, Merck) were used as buffer materials according to Britton and Welford.[31] Deionized water was distilled twice in a quartz column and HCl (1 N titrisol, Merck) was used for acidification.

Absorption spectra were recorded on a Unicam SP 8000 spectrophotometer with 1.0-cm matched quartz cells. Acidic solutions were obtained by using 1×10^{-4} M HCl; basic solutions were obtained by adding 4×10^{-4} M NaOH. Steady-state fluorescence spectra together with fluorescence yields (ϕ_f) and photochemical trans/cis isomerization were measured with a Shimatzu RF 510 spectrofluorometer. Fluorescence intensities were measured at right angle to the exciting light. Narrow excitation slits were used in order to minimize the intensity of the exciting light and thus to keep the isomerization reaction at low rate. Photochemical trans/cis isomerization quantum yields (ϕ_{tc} and ϕ_{ct}) were determined by irradiating the dye solutions in cylinderical cuvettes of 3 mL volume and 10 mm optical path length with a xenon lamp (150 W) using the spectrofluorometer at 366 nm as a monochromatic irradiation source. For quantum yield calculations, the method of Gauglitz[29,32-34] was used. The intensity of the irradiation incident light was measured by using the ferrioxalate actinometer, which is described by Hatchard and Parker.[35] Fluorescence quantum yields were based on quinine bisulfate in 1 N H_2SO_4 as spectral and quantum standard (ϕ_f = 0.55 at λ_{ex} = 366 nm).[36]

(b) Theoretical Method. The atom superposition and electron delocalization molecular orbital (ASED-MO) method[37] used in this paper is a semiempirical theoretical approach based on partitioning molecular charge density distribution functions (ρ_{mol}) into rigid atomic components and a nonrigid or nonperfectly following (ρ_{npf}) component. For a diatomic molecule ab as example

$$\rho_{mol} = \rho_a + \rho_b + \rho_{npf} \qquad (1)$$

where ρ_a and ρ_b are atomic charge densities centered on nucleus a and nucleus b and ρ_{npf} is an electron delocalization or bond charge density. From the electrostatic theorem, the force on nucleus a has two nonzero components, an attractive force due to ρ_{npf} and a repulsive one due to ρ_b on nucleus b. These forces are integrated, yielding the potential energy $E(R)$, where R is the internuclear distance:

$$E(R) = E_r(R) + E_{npf}(R) \qquad (2)$$

$E_r(R)$ is the repulsive energy due to atom superposition and $E_{npf}(R)$ is the attractive energy due to electron delocalization. The $E_r(R)$ function is determined with Slater atomic orbitals from the literature.[38] E_{npf} is approximated as the difference between the valence electron orbital energies for the atoms calculated from measured first ionization potentials[39] and the molecular orbital energies of the valence electrons in the molecule. The molecular orbital energies are functions of the atomic ionization potentials, Slater orbital exponents, and molecular structure as calculated by using a modified extended Hückel Hamiltonian. In heteronuclear systems we take charge self-consistency into account in an approximate way, by systematically adjusting the ionization potential and orbital exponent parameters until the charge transfer and bond length of the diatomic molecule are reasonable. When the orbital energy difference approximation is used for E_{npf}, the charge density function of the more electronegative atoms is usually used to provide the density function for E_r. The ASED-MO theory has been applied to numerous diverse studies of molecular structures, reaction mechanisms, and electronic and vibrational properties.

TABLE I: Atomic Orbital Parameters: Principal Quantum Number (*n*), Ionization Potential (IP) (eV), and Orbital Exponents (ζ) (au)

	s			p		
atom	*n*	IP	ζ	*n*	IP	ζ
N	2	18.33	1.924	2	12.53	1.917
O	2	28.48	2.246	2	13.62	2.227
C[a]	2	16.59	1.658	2	11.62	1.618
H	1	13.60	1.20			

[a] As discussed in the text, Slater exponents for the carbons (C_8,C_{10}) and (C_5,C_9) are 1.858 and 1.818.

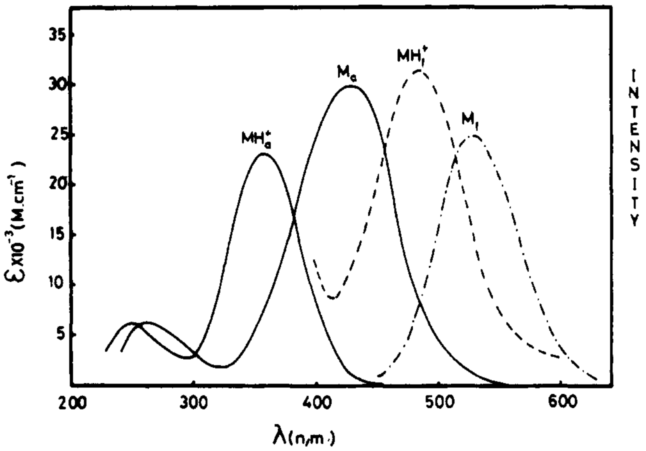

Figure 1. Absorption and fluorescence spectra of 2.0×10^{-5} M/L aqueous solutions of the dye in both acidic (pH = 6) and basic (pH = 10) forms, handled only in the dark: MH_a^+, M_a are absorption spectra; MH_f^+, M_f are fluorescence spectra.

The atomic parameters used for C, H, N, and O in all calculations in this paper are summarized in Table I. The Slater exponents of 2s and 2p of (C_8,C_{10}) and (C_5,C_9) are increased by 0.20 au from the atomic values of Clementi and Raimondi[38b] to provide reasonable M and MH$^+$ structures, respectively. Because of ionicity, the ionization potentials for N are decreased by 2.0 eV from the atomic values.[39a] In all reported results for equilibrium structure, all bond lengths between C, N, and O atoms are optimized by the variational theorem to the nearest 0.01 Å. A planar geometry was assumed for the trans structure. Bond lengths of C–H bonds are kept constant and bond angles are fixed to 120° in the calculations.

Results and Discussion

Spectroscopic Characterization and Protolytic Equilibrium. The longest wavelengths of absorption and fluorescence spectra of our merocyanine dye were measured experimentally in aqueous solution (Figure 1). For a solution of 1×10^{-3} M NaOH, the dye molecules are completely unprotonated, M (basic form). The longest electronic absorption band maximum is at 426 nm and its steady-state fluorescence band maximum is at 515 nm. For a solution of 1×10^{-4} M HCl, the dye molecules are completely protonated, MH$^+$ (acidic form). The longest electronic absorption band maximum is at 362 nm and its steady-state fluorescence band maximum is at 485 nm. An extinction coefficient ϵ of 30 $\times 10^3$ L mol^{-1} cm^{-1} at 425 nm is calculated for the basic solution and 22 $\times 10^3$ L mol^{-1} cm^{-1} at 360 nm for the acidic solution. Measurements of absorption and fluorescence spectra of the protonated dye were handled only in the dark to avoid the photochemical trans/cis isomerization reaction which is very

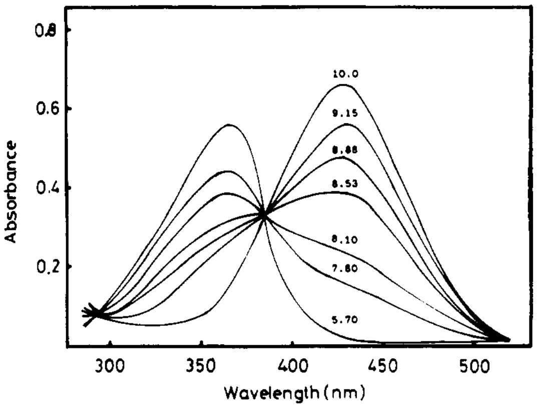

Figure 2. Absorption spectra of aqueous solutions, 2.0 × 10⁻⁵ M/L of the dye at different pH values handled only in the dark.

sensitive even to diffuse light. This point will be discussed later. In general, the fluorescence intensity of solutions of M and MH^+ was found very weak at room temperature. The fluorescence quantum yield of the acidic form, 6×10^{-4}, is somewhat larger than that of the basic form, 1.5×10^{-4}.

Absorption spectra of M and MH^+ which exhibit two overlapping bands represent a simple protolytic equilibrium of only two forms. The equilibrium constant could be determined spectrophotometrically by measuring the absorption spectra of the dye at different pH values. Figure 2 shows a sharp isosbestic point when the solutions were handled only in the dark. From these spectra, the pK_a value was calculated at 25 °C as 8.4. Kuder[40] has discussed the validity of the Förster cycle for stilbazolium betaines and compared the results with the data reported for phenol and 1- and 2-naphthol. Accordingly, the Förster cycle[41-43] was applied for determining the excited-state dissociation constant. The difference between pK_a of ground and excited state is given as

$$\Delta pK = pK_a - pK_a^* = hc(\nu_a - \nu_b)/2.303kT = (2.1 \times 10^{-3})(\nu_a - \nu_b)$$

at 25 °C. ν_a and ν_b are frequencies in cm^{-1} of 0–0 electronic transitions of acidic and conjugate basic forms of the dye. Data of absorption maxima, 362 and 426 nm, and of fluorescence maxima, 484 and 515 nm, were applied. The average values of the absorption and fluorescence energies, which are intermediate values, are used for the ΔpK_a determination. The value of ΔpK_a obtained is 5.66, which was used to calculate the dissociation constant of the dye, $pK_a^* = 2.74$ in the lowest excited singlet state. This value reveals that this type of compound is more acidic in the excited state than in the ground state as would also be expected on the basis of the theoretical calculations described below.

Photoisomerization of MH^+ Form. As discussed before, one should expect that the benzenoid resonance structure of our dye is a stilbene-like structure and could suggest the possibility of a photochemical trans/cis isomerization. According to Steiner et al.[28,44] and our studies, which have been reported about the photoisomerization reaction of a protonated merocyanine dye of stilbazolium betaine,[29,45-49] the absorption band of the protonated trans MH^+ was recorded before and after irradiation at 366 nm by using light intensity of 2.0×10^{-10} einstein/(cm^2 s). Figure 3a shows the spectral change of a MH_t^+ solution prepared in the dark upon 30 min of irradiation. The decrease of the absorbance of the longest wavelength until the photostationary state is reached concomitant with the increase of the absorbance of the shorter wavelength band at 240 nm is an indication of the occurrence of the photoisomerization reaction. The absorption spectrum of the pure cis form, Figure 3c, was obtained by calculating its extinction coefficient using the modified Blank and Ross method.[28,50] The calculation yields ϵ(366 nm) = 6.0×10^3 L mol^{-1} cm^{-1}. The photostationary state spectrum, Figure 3b, allows calculation of the percentage of cis form. The calculated ratio of cis to trans isomers was found to be 72:28. The time dependence of the absorbance on irradiation and the last values of light intensity and ϵ of trans and cis were used to give the individual $\phi_{t\rightarrow c}$ and $\phi_{c\rightarrow t}$ as 0.230 and 0.303, respectively. These values are found independent of oxygen or of the concentration of MH^+.

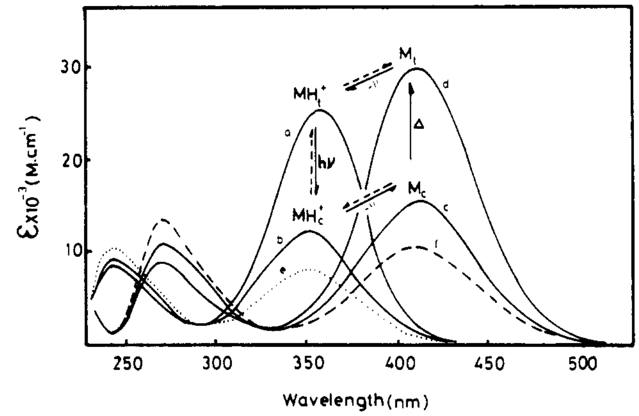

Figure 3. Absorption spectra showing the four stages of the reaction cycle: (a) 2.0 × 10⁻⁵ M/L aqueous solution of the dye, prepared in the dark, with 1 drop of 1 N HCl; (b) photostationary state obtained after irradiation at 366 nm; (c) after addition of 1 drop of 1 N NaOH to the cuvette; (d) spectrum of the unprotonated form as a result of the thermal reaction; (e) and (f) calculated spectra of pure cis form MH^+ and M, respectively.

Steiner[28] has noticed that there is an analogy in the structure of the protonated merocyanine dye and stilbene[51-57] in their photochemical trans/cis isomerization reaction and in quantum yield data. It was suggested that a phantom state is present in the protonated form at a 90° twisted conformation of the excited state by which the deactivation process can occur to either trans or cis ground state with a lifetime shorter than 5 ns. In contrast to MH^+, ϕ_{tc} of M is zero suggesting that there is a predominant contribution of a nonpolar resonance quinonoid structure with the absence of the central double bond which is necessary for the isomerization process.

Thermal Reactivity of the Cis Isomer M_c. The deprotonation process of the thermally stable MH_c^+ form leads to a deprotonated cis form, Figure 3c. The torsional stability of the central C–C bond is strongly decreased and the structure exists more in a quinonoid form offering the possibility of a thermal cis → trans isomerization reaction. It is a first-order reaction, and its rate constant k_{ct}, which is independent of the concentration, was found strongly temperature dependent. k_{ct} could be kinetically measured in the temperature range 30–67 °C. Applying the Arrhenius equation, the activation energy $E_a^{\ddagger}$ and the frequency factor k_0 of the reaction were evaluated. Also, the thermodynamic parameters of the reaction were calculated by using the Eyring theory.[58] The data at 25 °C are

$$\Delta G^{\ddagger}_{ct} = 24.07 \text{ kcal/mol} \qquad E_a^{\ddagger} = 28.15 \text{ kcal/mol}$$

$$\Delta H^{\ddagger}_{ct} = 27.56 \text{ kcal/mol} \qquad k_{ct} = 1.37 \times 10^{-5}\ s^{-1}$$

$$\Delta S^{\ddagger}_{ct} = 11.66 \text{ eu/mol} \qquad k_0 = 6.0 \times 10^{15}\ s^{-1}$$

The data obtained for the thermal reaction show that the activation energy is relatively large and the activation entropy change is also high. Although a high activation energy of the thermal reaction was found, a relatively fast reaction was noticed. This may due to the influence of the high activation entropy as mentioned by Steiner.[44] The high value of the activation energy obtained for the thermal reaction is strongly related to the high stability of the structure with C–C double bond character (benzenoid structures). The high activation entropy value leads to increase the disorder of the dye molecule with the surrounding

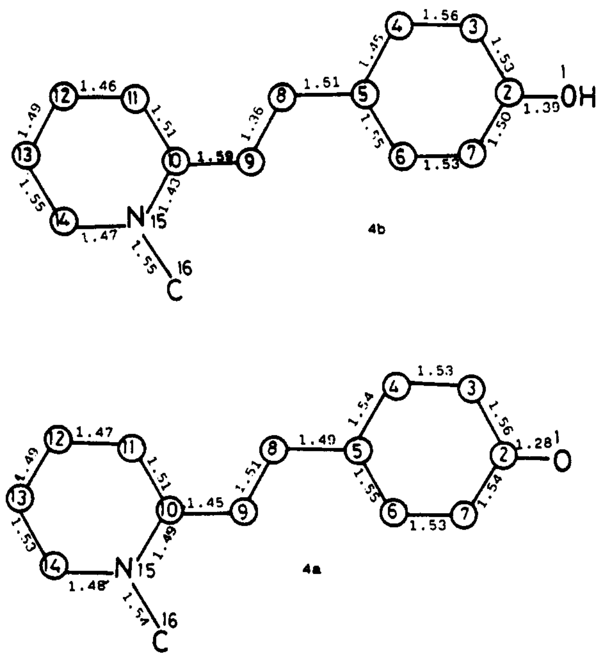

Figure 4. Bond lengths of the carbon skelton: (a) for M; (b) for MH$^+$. Resulting from ASED-MO calculations. The distances are given in Å.

solvent molecules. The benzenoid structure of the M dye has a relatively high dipole moment. The twisted configuration of the M molecule at 90° has a small dipole moment which is probably due to the contribution of the C–C single bond (the quinonoid structures). Moreover, at 90° twisted configuration the polar solvent molecules are less oriented toward the weak dipole field of the quinonoid structure but the polar solvent molecules are highly oriented toward the strong dipole field of the benzenoid structure. From the results of our protolytic, photochemical and thermal reactions, one can consider the above reactions as a complete molecular reaction cycle (Scheme II) similar to what was reported by Steiner.[28,44] The reaction cycle in Scheme II proceeds in one direction due to irreversibility of the thermal step in aqueous solution. This reaction cycle may explain the role of the protonated Schiff base of retinal in the light-driven proton pump[59] in the purple membrane of *Halobacterium halobium*.[60]

SCHEME II

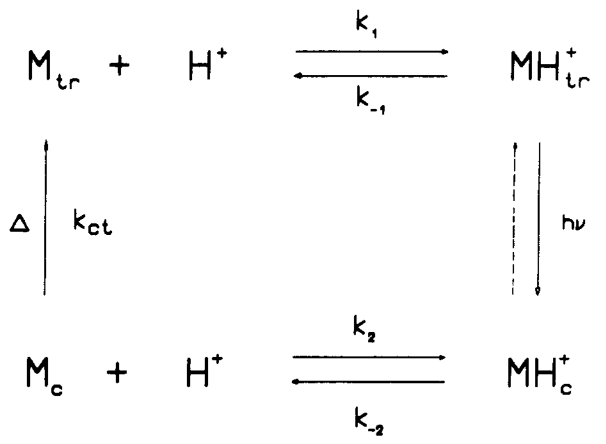

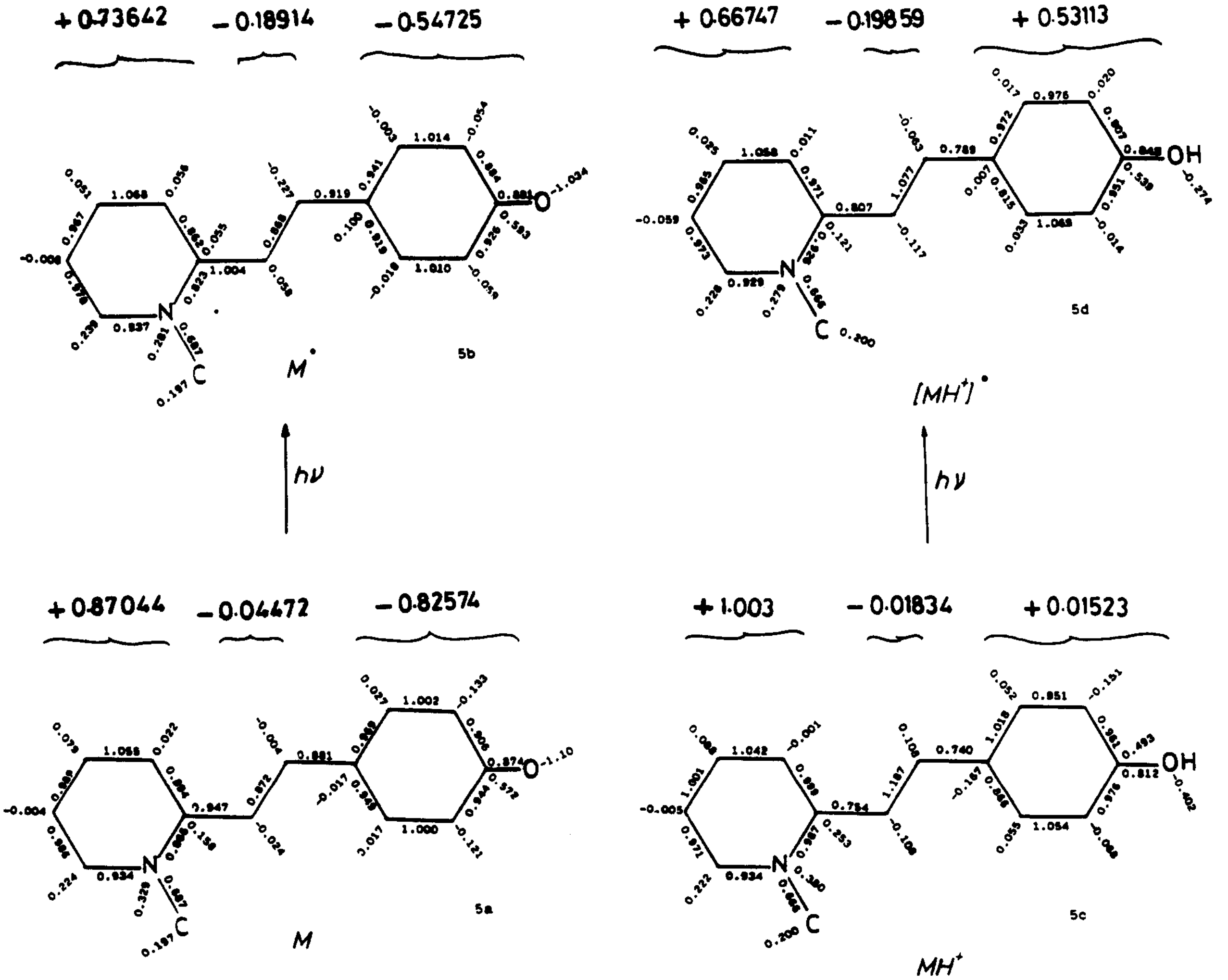

Figure 5. Atomic charge densities (values of the whole molecule including that of hydrogen atoms) and bond order: (a, b) for M in ground and excited states; (c, d) for MH$^+$ in ground and excited states.

ASED-MO Calculations. The optimized molecular structures of stilbazolium betaine M and MH^+ are shown in parts a and b of Figure 4, respectively. These calculations show that the bond lengths for M match the quinonoid valence structure whereas the geometry of the protonated compound MH^+ corresponds to the benzenoid structure. The bond lengths of the polymethine chain are inverted on going from unprotonated to protonated forms. Upon protonation the central C_8–C_9 bond length is reduced from a value of 1.51 Å, corresponding to a polyene-type single bond, to 1.36 Å, which is typical of a polyene double bond. Contrarily, the neighboring double bonds in the case of the M structure are stretched, from 1.49 to 1.61 Å, for the C_5–C_8 bond, and from 1.45 to 1.59 Å, for the C_9–C_{10} bond, upon protonation. Moreover the C_2–O bond length is characterized by extension from 1.28 Å for M to 1.39 Å for MH^+. The ring bond lengths show the expected alternation in the quinonoid structure M with shift toward a benzenoid structure upon protonation.

Our calculations suggest that the unprotonated dye has a stronger dipole moment than the protonated one. They also show the net charges and bond order of the stilbazolium betaines M and MH^+, respectively, in the ground state and lowest excited state. The distributions of positive and negative charges over the whole skelton of M and MH^+, which generates dipolar contributions, are different. In the ground state, a polar structure is shown for M with a positive charge of +0.87 e on the pyridinium moiety and a negative charge of −0.83 e on the phenoxy moiety, Figure 5a. Although the positive charge on the protonated form is delocalized over the whole molecule, most of it is localized on the pyridinium ring, as in Figure 5c. This explains a lower apparent molecular dipole moment for MH^+. Also, it is seen that, upon protonation in the ground state, a considerable loss of electron density occurs from the negative end (oxygen atom), from −1.10 e to −0.402 e, accompanied by gaining a charge on the positive end (nitrogen atom), from +0.329 e to +0.380 e. Upon excitation, the charge density on oxygen atom of MH^+ decreases from −0.402 to −0.274 e. This calculated decreasing of charge on the oxygen may explain increasing acidity of MH^+ in the excited state. Parts b and d of Figure 5 show the effect of excitation on the charge distribution and bond order of M and MH^+. In the case of the M structure, the excitation results in a different alternation of positive and negative charges on the phenoxy and pyridinium moieties. The negative charge, −0.826 e, localized on the phenoxy moiety is strongly reduced to −0.547 e and the positive charge localized on the pyridinium moiety is reduced from +0.870 e to +0.736 e. This agrees with the postulated decreasing of the molecular dipole moment of M upon excitation. Contrarily, the calculated charge distribution change of MH^+ is different. The positive charge on the phenoxy moiety strongly increases from +0.015 e to +0.531 e and the positive charge localized on the pyridinium moiety decreases from +1.00 e to +0.667 e. This agrees with the postulated increase of the effective molecular dipole moment. The changes of the calculated bond order on excitation correspond to the increased contribution of quinonoidal resonance structure of M and MH^+. The bond order of C_8–C_9, in the case of M, decreases from 0.872 to 0.868 whereas C_5–C_8 and C_9–C_{10} bond orders increase from 0.881 and 0.947 to 0.919 and 1.004, respectively. Also, in case of MH^+, the bond order of C_8–C_9 decreases from 1.187 to 1.077 and C_5–C_8 and C_9–C_{10} increase from 0.740 and 0.754 to 0.789 and 0.807, respectively.

We used ASED-MO calculations to investigate the nature of the electronic transitions and calculate their energies for the unprotonated and protonated stilbazolium betaine. The calculated orbital energies and structures of M and MH^+ are shown in Figure 6. The calculations show that the lowest energy transition in both structures is $\pi \rightarrow \pi^*$ which is mainly described by one electron excitation from the highest occupied molecular orbital (HOMO), significantly localized on C_5 and C_9 to the lowest unoccupied molecular orbital (LUMO), with a considerable contribution from C_8 and C_{10}. The calculated excitation energies are 1.45 and 2.40 eV for M and MH^+, respectively. The calculations indicate a further excitation with energies of 2.56 eV in the case of M and 3.29 eV in the case of MH^+, which is due to a transition from the oxygen lone-pair orbital shown in Figure 6 (with a large amplitude on oxygen atom), to the LUMO with complete π^* character. We can define these transitions as the lowest $n \rightarrow \pi^*$ transitions. Also, there is another possible transition $\sigma \rightarrow \pi^*$ with excitation energies of 3.50 and 4.29 eV in the cases of M and MH^+, respectively.

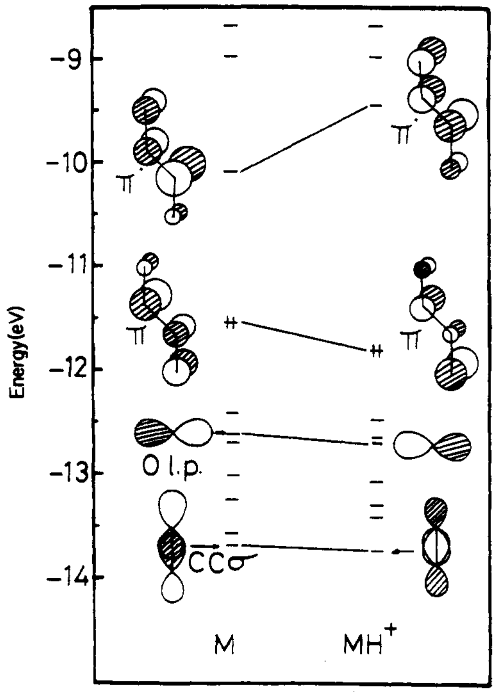

Figure 6. Correlation diagram for M and MH^+ molecular orbitals: O l.p., oxygen lone pair; ++, HOMO. The orbital coefficients are only given for the central part of the molecule.

The protonation of M in the ground state is an exothermic reaction (eq 3). Correspondingly, MH^+ was found 6.62 eV more

$$M + H^+ \rightleftharpoons MH^+ \qquad (3)$$

stable than M. Although the calculated energy difference is overestimated as compared to the measured value, due to the structural parameters used in this work, this value shows the higher stability of the protonated stilbazolium betaine. In the excited state, in case of the lowest $\pi \rightarrow \pi^*$ transition, MH^+ becomes more acidic. The higher stability of MH^+ in the ground state with respect to M can be understood from Figure 6. Upon protonation, the CC π orbital energy is stabilized by 0.3 eV while the counterpart π^* orbital becomes more destabilized by 0.64 eV. The lengthening of the C–O bond due to protonation of the M form would cause a slight stabilization of the oxygen lone-pair orbital and the CC σ orbital.

Acknowledgment. The authors wish to thank Ms. El-sayda Amerah for typing the manuscript and Mr. Fawzy T. Abdel-Halim for his expert drawings. We also express our appreciation to a reviewer for insightful comments.

References and Notes

(1) Grinwald, A.; Frostig, R. D.; Lieke, E.; Hildesheim, R. *Phys. Rev.* **1985**, *8*, 263.

(2) Loew, L. M.; Scully, S.; Simpson, L.; Waggoner, A. S. *Nature* **1979**, *281*, 497.

(3) *Nonlinear Optical Properties of Organic and Polymeric Materials*; Williams, D. J., Ed.; ACS Symposium Series 233; American Chemical Society: Washington, DC, 1983.

(4) Horie, H.; Hirao, K.; Kenmochi, N.; Mita, I. *Makromol. Chem., Rapid Commun.* **1988**, *9*, 267.

(5) Takahashi, K.; Komura, T.; Imanoga, H. *Nippon Kagaku Kaishi* **1985**, *12*, 2226.

(6) Kirk-Othmer *Encycl. Chem. Technol.* **1985**, *6*, 122.

(7) Sieber, F.; Spivak, J. L.; Sutcliffe, A. *Proc. Natl. Acad. Sci. U.S.A.* **1984**, *81*, 7584.

(8) Arden, W.; Fromherz, P. *J. Electrochem. Soc.* **1980**, *127*, 372.

(9) Inacker, O.; Kuhn, H.; Möbius, D.; Debuch, G. *Z. Phys. Chem.* **1976**, *101*, 337.

(10) Brooker, L. G. S.; Keyes, G. H.; Heseltine, D. W. *J. Am. Chem. Soc.* **1951**, *73*, 5350.

(11) Hünig, S.; Rosenthal, O. *Justus Liebigs Ann. Chem.* **1955**, *161*, 592.

(12) Abdel-Halim, S. T. *J. Chem. Soc., Faraday Trans.* **1993**, *89*, 55.

(13) (a) Dimroth, K.; Reichardt, C.; Siepmann, T.; Bohlmann, F. *Justus Liebigs Ann. Chem.* **1963**, *661*, 1. (b) Dimroth, K.; Reichardt, C. *Justus Liebigs Ann. Chem.* **1969**, *93*, 727. (c) Maksimouie, Z. B.; Reichardt, C.; Spiric, A. *Z. Anal. Chem.* **1974**, *100*, 270.

(14) Kamlet, M. J.; Abboud, J. L.; Abraham, M. H.; Taft, R. W. *J. Am. Chem. Soc.* **1977**, *99*, 6027.

(15) Kamlet, M. J.; Abboud, J. L.; Abraham, M. H.; Taft, R. W. *J. Org. Chem.* **1983**, *48*, 2877.

(16) Kamlet, M. J.; Abboud, J. L.; Abraham, M. H.; Taft, R. W. *Prog. Phys. Org. Chem.* **1981**, *13*, 485; *J. Am. Chem. Soc.* **1981**, *103*, 1080.

(17) (a) Lippert, E.; Moll, F. *Ber. Bunsen-Ges. Phys. Chem.* **1954**, *58*, 718. (b) Lippert, E. *Ber. Bunsen-Ges. Phys. Chem.* **1957**, *61*, 962. (c) Buncel, E.; Rajagopal, S. *Acc. Chem. Res.* **1990**, *23*, 226.

(18) Dähne, S.; Schole, F.; Nolte, K. D. *Z. Chem.* (*Leipzig*) **1973**, *13*, 471.

(19) Benson, H. G.; Murrell, J. N. *J. Chem. Soc., Faraday Trans.* **1972**, *2*, 137.

(20) Botrel, A.; Beuze, A.; Jacques, P.; Strube, H. *J. Chem. Soc., Faraday Trans. 2* **1984**, *80*, 1235.

(21) Tavan, P.; Schulten, K. *Chem. Phys. Lett.* **1984**, *110*, 191.

(22) Tavan, P.; Schulten, K.; Oesterheld, D. *Biophys. J.* **1985**, *47*, 415.

(23) Orlandi, G.; Schulten, K. *Chem. Phys. Lett.* **1980**, *64*, 370.

(24) Platt, J. R. *J. Chem. Phys.* **1956**, *25*, 80.

(25) Stoeckenius, W.; Bogomolni, R. *Annu. Rev. Biochem.* **1982**, *51*, 587.

(26) Bartocci, G.; Bortolus, P.; Mazzucato, U. *J. Phys. Chem.* **1973**, *77*, 605.

(27) Schulte-Frohlinde, D.; Güsten, H. *Justus Liebigs Ann. Chem.* **1971**, *49*, 749.

(28) Steiner, U.; Abdel-Kader, M. H.; Fischer, P.; Kramer, H. E. A. *J. Am. Chem. Soc.* **1978**, *100*, 3190.

(29) Abdel-Kader, M. H.; Hamzah, R. Y.; Abdel-Halim, S. T. *Photochem. Photobiol.* **1989**, *50*, 599.

(30) Minch, M. J.; Shah, S. J. *J. Chem. Educ.* **1977**, *54*, 709.

(31) Britton, Welford *J. Chem. Soc.* **1937**, 1848.

(32) Gauglitz, G. J. *Photochemistry* **1976**, *5*, 41.

(33) Frank, R.; Gauglitz, G. J. *Photochemistry* **1977**, *7*, 355.

(34) Gauglitz, G.; Hubig, S. J. *Photochemistry* **1981**, *15*, 255.

(35) Hatchardt, J. G.; Parker, C. A. *Proc. R. Soc. London, Ser. A* **1956**, *235*, 815.

(36) Melhuish, W. H. *J. Phys. Chem.* **1961**, *65*, 229.

(37) Anderson, A. B. *J. Chem. Phys.* **1975**, *62*, 1187.

(38) (a) Richardson, J. W.; Nieuwpoort, W. C.; Powell, R. R.; Edgell, W. F. *J. Chem. Phys.* **1962**, *36*, 1057. (b) Clementi, E.; Raimondi, D. L. *J. Chem. Phys.* **1963**, *38*, 2686. (c) Basch, H.; Gray, H. B. *Theor. Chim. Acta* **1966**, *4*, 367.

(39) (a) Lotz, W. *J. Opt. Soc. Am.* **1970**, *60*, 206. (b) Moore, C. E. *Atomic Energy Levels*; National Bureau of Standards Circular (U.S.) 467; U.S. Government Printing Office: Washington, DC, 1958.

(40) Kuder, J. E.; Wychik, D. *Chem. Phys. Lett.* **1974**, *24*, 69.

(41) Förster, Th. *Z. Electrochem.* **1950**, *54*, 42.

(42) Jaffè, H. H.; Jones, H. L. *J. Org. Chem.* **1965**, *30*, 964.

(43) Vander Donckt, E. *Prog. Reaction Kinet.* **1966**, *5*, 273.

(44) Abdel-Kader, M. H.; Steiner, U. E. *J. Chem. Educ.* **1983**, *60*, 160.

(45) Abdel-Halim, S. T. M.Sc. Thesis, Tanta University, Egypt, 1982.

(46) Abdel-Mottaleb, M. S. A.; Abdel-Kader, M. H.; Abdel-Halim, S. T. *Int. Conf. Photochem. Photobiol., II* **1983**, 1329.

(47) Abdel-Kader, M. H.; Hamzah, R. H.; Abdel-Halim, S. T. *Colloids Surf.* **1988/1989**, *34*, 133.

(48) Abdel-Halim, S. T. Ph.D. Thesis, Tanta University, Egypt, 1986.

(49) Abdel-Halim, S. T.; Abdel-Kader, M. H.; Steiner, U. E. *J. Phys. Chem.* **1988**, *92*, 4324.

(50) Blanc, J.; Ross, D. L. *J. Phys. Chem.* **1968**, *72*, 2817.

(51) Saltiel, J. *J. Am. Chem. Soc.* **1967**, *89*, 1036.

(52) Saltiel, J.; Megarity, E. D. *J. Am. Chem. Soc.* **1972**, *94*, 2742.

(53) Orlandi, G.; Siebrand, W. *Chem. Phys. Lett.* **1975**, *30*, 352.

(54) Whitten, D. G.; Lee, Y. J. *J. Am. Chem. Soc.* **1972**, *94*, 9142.

(55) Schulte-Frohlinde, D.; Blume, H.; Güsten, H. *J. Phys. Chem.* **1962**, *66*, 2486.

(56) Courtney, S. H.; Fleming, G. R. *J. Chem. Phys.* **1985**, *83* (1), 215.

(57) Waldeck, D. H. *Chem. Rev.* **1991**, *91*, 415.

(58) Eyring, H. *Chem. Rev.* **1935**, *17*, 65.

(59) Schulten, K.; Tavan, P. *Nature* (*London*) **1978**, *85*, 272.

(60) Oesterheld, D.; Stoeckenius, W. *Proc. Natl. Acad. Sci. U.S.A.* **1973**, *70*, 2853.